Proc. Estonian Acad. Sci. Phys. Math., 1995, 44, 2/3, 252–265
https://doi.org/10.3176/phys.math.1995.2/3.15

ORIGIN OF GAP ANISOTROPY AND PHONON RENORMALIZATION

Andreas BILL[a], Vladimir HIZHNYAKOV[b], and Ernst SIGMUND[a]

[a] Institut für Physik, Technische Universität Cottbus (Technical University of Cottbus), Postfach 101344, 03013 Cottbus, Deutschland (Germany)

[b] Tartu Ülikool (University of Tartu), Tähe 4, EE-2400 Tartu, Eesti (Estonia); Eesti Teaduste Akadeemia Füüsika Instituut (Institute of Physics, Estonian Academy of Sciences), Riia 142, EE-2400 Tartu, Eesti (Estonia)

Received 2 December 1994, accepted 17 April 1995

Abstract. The anisotropy of a superconducting gap is studied for two different hole–lattice interactions characteristic of high-T_c superconductors. The first one is the short-range distortive coupling and the second one, the long-range part due to imperfect screening of the Coulomb potential. Then the influence of different symmetries (s wave, d wave...) of the gap on the renormalization of $\mathbf{q} \to 0$ phonons is studied. The results are compared with Raman measurements. Conclusions about the symmetry of the gap and the strength of the hole–lattice coupling in high-T_c materials are presented.

Key words: superconductivity, gap anisotropy, $s(d)$-wave pairing, phonon renormalization.

1. INTRODUCTION

One of the most characteristic features common to all cuprate high-T_c superconductors is the existence of doping-dependent *local inhomogeneities* observed both in the electronic and the lattice subsystem. In the first instance it was theoretically proposed [1, 2] and experimentally observed [3, 4] that the long-range antiferromagnetic (AF) ordering is locally destroyed upon doping perovskites (electronic phase separation (PS)). In the second case, several experiments [5–7] have shown that the local structure of the lattice strongly deviates from the one imposed by the average crystal symmetry. These facts give hints on the structure and the dimension of quasiparticles (dressed holes), which determine the properties of the normal and the superconducting state. Below we discuss how these inhomogeneities are related to electron–lattice interaction and what the consequences are for the anisotropy of a superconducting gap and the renormalization of the phonon energy below T_c.

The first aspect considered here has a purely electronic character. It concerns the existence of microscopic inhomogeneities in the magnetic structure of CuO_2 planes. All cuprate systems show an AF ordering of Cu spins below the Neel temperature T_N in an undoped case. When doping or oxidizing a parent compound of a high-T_c superconductor (e.g. La_2CuO_4, $YBa_2Cu_3O_6$ ...), holes appear in CuO_2 planes. It has been shown in the framework of mean-field approximations (Hartree–Fock and slave-bosons) of the three-band Hubbard model [2, 8] that doped holes destroy locally the AF order through the formation of spin-polarized clusters. One such magnetic quasi-particle is made up of about five to ten polarized Cu spins. The dynamics of a hole is here determined by free motion inside the cluster, whereas the last hole is hardly mobile. The ever more doping of the system leads to an increase of the hole concentration in the planes and the clusters begin to overlap. Then the charge carriers move into the low-dimensional ($d \leq 2$) metal-like network formed this way. Above a critical concentration (percolation threshold) the clusters percolate and conductivity or superconductivity sets in. In this picture the system undergoes a *percolative phase separation* both in hole-rich and hole-poor domains. An important feature of this PS is that, in contrast to the chemical phase separation (clustering of excess oxygens), it is driven by a pure electronic mechanism. For a review on PS see [4, 9].

The second aspect that gives hints on what kind of quasiparticles are formed in high-T_c compounds concerns the lattice structure. It has been observed by neutron diffraction [5, 10], EXAFS [6] or NQR [7] that for most of the doped cuprate systems the local structure of the system differs from the average crystal symmetry in some concentration range. CuO_6 octahedras are tilted along different axes [5] and the Cu–O(4) bond (apex oxygen) shows two typical distances [6, 7]. All these effects can be seen to be related to the presence of holes in the plane and to some extent on the apex oxygen. Furthermore, they are believed to be dynamic rather than static in the sense that they are correlated to the particles' motion. From the dimension of lattice inhomogeneities (several unit cells) one can infer that holes form intermediate polarons containing five to ten Cu atoms [11]. This is in full agreement with the concept of spin-polarized clusters and with the fact that holes can move only in a low-dimensional network, since it can be shown that the intermediate polaron is the only stable quasiparticle in this case. The dynamics of a hole with respect to lattice deformations is thus given by the hole's ability to move through the crystal, whereby an important part of its polarization is carried with it.

An analysis of the structure of high-T_c superconductors presented above shows that they have characteristic features that do not occur in usual metals. This is reflected in the properties of the hole–lattice interaction. In the low- and the intermediate doping regime we assume that holes move in a quasimetallic percolation network imbedded in the insulating AF system. Thus the particles interact mainly with the ions of the insulating domains, which results in an essential coupling to optical modes. Furthermore, the

ionic character of high-T_c compounds implies that the main contribution to short-range hole–lattice interaction comes from the variation of the site and Cu–O hopping energies. Since the holes are primarily located on the oxygens in CuO_2 planes, they are situated on noncentrosymmetrical positions of the crystal. As a consequence, as observed, they can induce static distortions of the lattice in their near surrounding.

In addition to the short-range part of interaction there is an important long-range contribution to the coupling as well. This follows from the fact that the concentration of charge carriers (holes) is small in these systems and that they are low-dimensional systems. Consequently, there is an incomplete screening of hole–lattice interaction in cuprate superconductors and the long-range part must be taken into account.

The hole–lattice interaction will be influenced in (at least) three respects upon changing the doping. Firstly, the increase of the hole concentration and thus of the dimensionality of the network ($d \rightarrow 2$) implies a better screening and a decrease of the long-range part of interaction. Secondly, the polaron becomes larger because of the growing of the allowed region in which the particle can move. For this reason, finally, it is mainly the nondiagonal (transitive) part of short-range hole–lattice interaction that will be affected by doping.

2. ANISOTROPY OF THE SUPERCONDUCTING GAP

The success of the BCS model (**k**-independent pairing potential $V_{\mathbf{k}\mathbf{k}'}$) for the description of conventional superconductors supports the experimental observation that in most of them the gap is almost constant in the whole Brillouin zone ($\Delta_{\mathbf{k}} \simeq \Delta$). In high-$T_c$ superconductors, however, it has been observed by ARPES [12] or PCS (point conduct spectroscopy) [13] that $\Delta_{\mathbf{k}}$ is strongly anisotropic. Anisotropy has two components. The first one is between the ab plane and the c direction and the second one, in the ab plane itself. In what follows we study only the structure and the symmetry of the second kind of anisotropy.

The superconducting gap is defined by $\Delta_{\mathbf{k}} = \sum_{\mathbf{k}'} V_{\mathbf{k}\mathbf{k}'} < c_{-\mathbf{k}'\downarrow} c_{\mathbf{k}'\uparrow} >$ and it is the solution of the BCS gap equation:

$$\Delta_{\mathbf{k}} = -\sum_{\mathbf{k}'} V_{\mathbf{k}\mathbf{k}'} D_{\mathbf{k}'} \quad \text{with} \quad D_{\mathbf{k}'} = \Delta_{\mathbf{k}'} \frac{\tanh\left(\frac{\beta E_{\mathbf{k}'}}{2}\right)}{2 E_{\mathbf{k}'}} \quad . \tag{1}$$

$E_{\mathbf{k}} = \sqrt{\varepsilon_{\mathbf{k}}^2 + \Delta_{\mathbf{k}}^2}$. From the definition of $\Delta_{\mathbf{k}}$ it is obvious that this function is k-independent if $V_{\mathbf{k}\mathbf{k}'}$ is k-independent. Thus, anisotropy is directly related to the pairing mechanism of quasiparticles (holes). On the other hand, the symmetry properties of the gap function are not only determined by $V_{\mathbf{k}\mathbf{k}'}$ but also in an essential way by the structure and the

filling of the band through $D_{\mathbf{k}}$ in (1). Here we consider the gap anisotropy in the ab plane for short-range and long-range interactions separately and study the symmetry properties of the solutions of the gap equation for different fillings of the band. For numerical calculations we consider one electronic band,

$$\varepsilon_{\mathbf{k}} = t\{2(\cos(k_x a) + \cos(k_y a)) - 4t_1 \cos(k_x a)\cos(k_y a) + 2t_2 \cos(k_z c) + \mu'\}, \quad (2)$$

taking into account the nearest (t) and the next-nearest (t_1) neighbour intralayer and the interlayer (t_2) hopping to fit correctly the band structure calculations for the $YBa_2Cu_3O_{7-\delta}$ system [14]. The parameters are set to $t = -0.25\,\text{eV}$, $t_1 = 0.45$, and $t_2 = 0.1$ [15, 16].

The short-range electron–lattice interaction is mainly of a distortive type and thus affects the near surrounding of the unit cell where the hole is located. The pairing induced by this interaction can be modelled by the following phenomenological potential:

$$V_{\mathbf{k}\mathbf{k}'} = V_1[\cos(q_x) + \cos(q_y)] + V_2 \cos(q_x)\cos(q_y), \quad (3)$$

($\mathbf{q} = \mathbf{k}' - \mathbf{k}$). The term in V_1 corresponds to the nearest neighbour and the one in V_2, to the next nearest neighbour hole–hole interaction. As one can see, the anisotropy of the gap for short-range interaction will be a *sign of the lattice structure* of the CuO_2 plane. From the structure of this function the possible solutions can have an s-wave as well as a d-wave symmetry (for definition see Sec. 3.2), depending on the values of the parameters. The constants V_1 and V_2 have been calculated for the interaction with optical modes and by taking into account the local Coulomb repulsion in a phenomenological way [17]. In Figs. 1 and 2 stable solutions of gap equation (1) for two different fillings are depicted. In the first case the Fermi surface is closed around the Γ point, whereas it is open in the second one. The gap resulting from this pairing potential shows a strong anisotropy with an s-wave and a d-wave symmetry, respectively. Only the second case can fit the experimental results (maxima at the points $(\pm\pi, 0), (0, \pm\pi)$ and minima along the lines $k_y = \pm k_x$; the gap was not measured at the centre of the Brillouin zone). Nevertheless, a more careful study of the gap equation is needed for this potential, since other types of solutions can be stable, too. Furthermore, a microscopic model for the holes and the phonons in CuO_2 planes has been studied in [18]. It has led to a pairing potential for which (1) has only s-wave solutions for the fillings studied.

The nontotally screened long-range hole–lattice interaction which is at least partly due to a microscopic phase separation and which corresponds to the interaction with long-wave optical modes, can be modelled by the potential [19]

$$V_{\mathbf{k}\mathbf{k}'} = \frac{V_c}{q_x^2 + q_y^2 + \kappa^2} \quad (4)$$

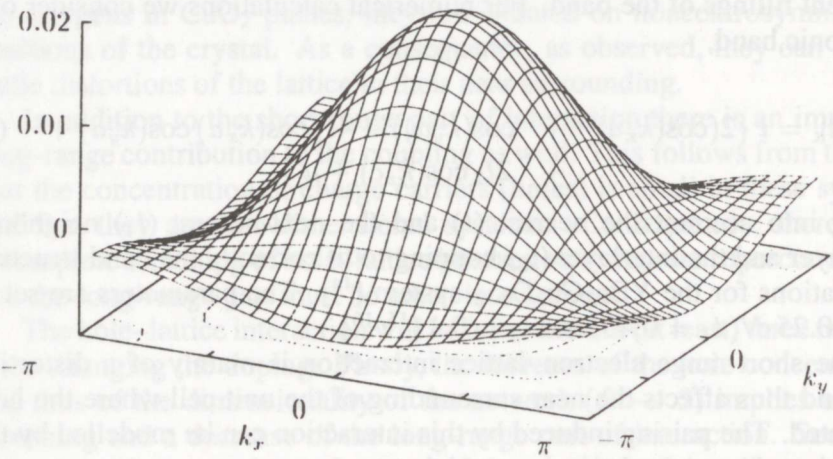

Fig. 1. Gap function at $T = 0$ for Eq. (3) with $V_1 = -0.19$, $V_2 = -0.34$, $\mu' = -2.22$. Energies are in meV. Equipotentials are shown in the (k_x, k_y) plane.

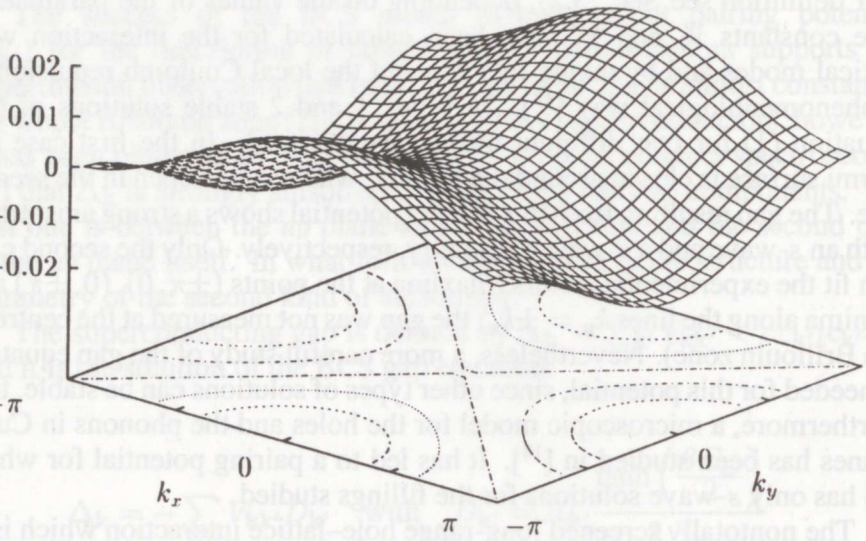

Fig. 2. Gap function at $T = 0$ for Eq. (3) with $V_1 = -0.29$, $V_2 = -0.52$, $\mu' = -1.35$. Energies are in meV.

with $\mathbf{q} = \mathbf{k}' - \mathbf{k}$. $\kappa(\ll k_F)$ is the screening factor of interaction and it depends on the concentration of doped holes. Since $V_{\mathbf{k}\mathbf{k}'}$ has a C_∞ symmetry axis perpendicular to the (k_x, k_y) plane in the Brillouin zone, the structure of the anisotropy of the gap is a *sign of the* $\mathbf{k}$ *dependence of the electronic density of states*. Again typical stable solutions for two fillings are depicted in Figs. 3 and 4.

As one can see, the solution for $\mu' = -1.35$ (which is the filling for which the ARPES experiments were done [12]) has the properties of the measured gap. One can also find d-wave-type solutions of the gap equation for the long-range hole–lattice interaction. However, for all the fillings studied the stable solution has an s-wave symmetry. The solutions were calculated only for one value of the doping-dependent screening factor κ. A more extensive study of the gap as a function of this parameter is in progress.

3. PHONON RENORMALIZATION BELOW T_c

It is generally recognized that the superconducting gap is strongly anisotropic in high-T_c materials. However, there is much controversy about the symmetry properties of the function (s wave, d wave or something else?). From the theoretical point of view this reflects the fact that the origin of the pairing mechanism is still an open question. Indeed, some theories predict an anisotropic gap function with a d wave [20], others with an s wave [15, 18, 19] and some with a mixed symmetry [21]. Since experimentally it is not possible at the present stage to unambiguously determine this symmetry, it is useful to find an indirect way to obtain information about the k dependence of the gap. One possibility is to study another peculiar property of high-T_c materials that is directly affected by the gap anisotropy, namely phonon renormalization below T_c. In what follows we give a general analytical derivation of this renormalization. We then study the influence of several types of anisotropies on the shift and the broadening of $\mathbf{q} = 0$ phonon lines and compare the results with those of Raman experiments.

The renormalization of the phonon energy below T_c is related to the fact that in the superconducting state the electronic density of states (DOS) is modified due to the appearance of a gap. To study how this change affects phonons let us suppose in the first step that the gap is constant, $\Delta_{\mathbf{k}} = \Delta$ (BCS model). In this case the DOS exhibits a gap of the width 2Δ and diverges at the upper edge of it. If 2Δ is much smaller than the characteristic phonon energy ω_c, one expects that the change of the DOS affects but weakly the phonon spectrum. This is the case encountered in most of the conventional superconductors. On the other hand, if 2Δ has the same order of magnitude as ω_c, the effect should be essential. This is the case of the high-T_c superconductors for which $2\Delta_{\max} \sim \omega_c$ (~ 30 meV for $YBa_2Cu_3O_7$). For these systems a phonon with the energy below 2Δ cannot

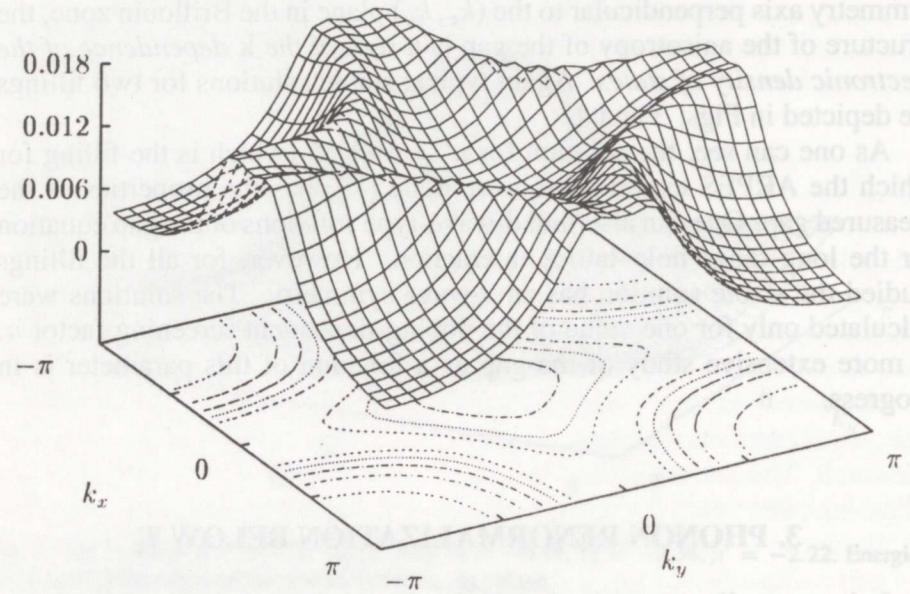

Fig. 3. Gap function at $T = 0$ for Eq. (13) with $V_c = -0.46$, $\mu' = -1.35$ and $\kappa = 0.3$. Energies are in meV.

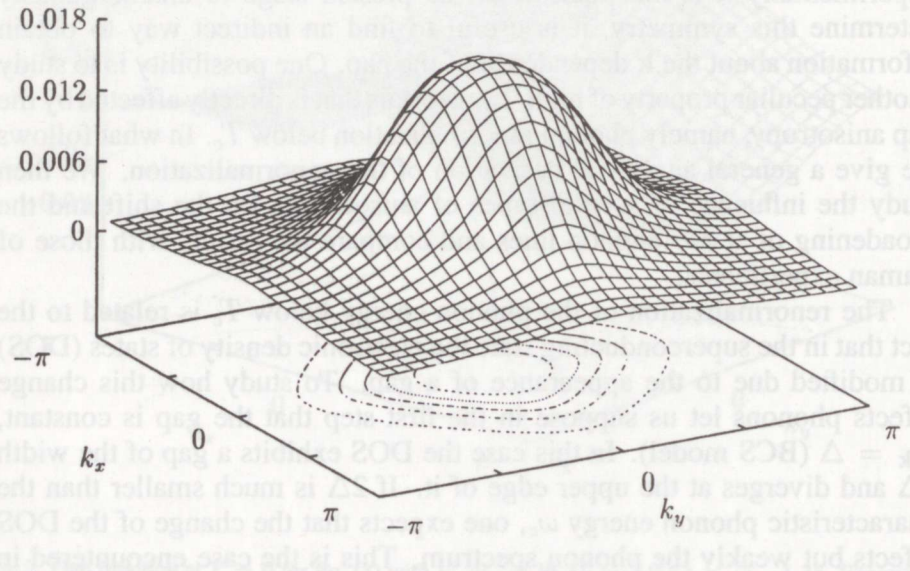

Fig. 4. Gap function at $T = 0$ for Eq. (13) with $V_c = -0.29$, $\mu' = -2.22$ and $\kappa = 0.3$. Energies are in meV.

scatter charge carriers of the superconducting condensate and the phonon line shifts to smaller energies without changing its width. In the opposite case new scattering channels are open in the electronic spectrum since the phonon energy is high enough to break Cooper pairs. This implies a broadening of the phonon line and a shift to higher energies. The nearer the phonon energy is to the gap 2Δ, the stronger the effect should be because the electronic DOS is singular at the upper edge of the gap. If one has a system with phonons' energy near 2Δ (some below and others above it), one can determine in this way the approximate value of the gap. This method has been used to estimate Δ in $RBa_2Cu_3O_7$ (R is rare earth) [22]. However, in these systems the gap is strongly anisotropic and the situation is thus more complicated than sketched above.

If the gap has a strong **k** dependence, the renormalization of the phonon energy will depend on the structure of anisotropy. This follows from the fact that the symmetry of the gap function affects the behaviour of the electronic DOS in the range $2\Delta_{max}$ around the Fermi energy ε_F. For example, the pure s-wave isotropic case presented above shows a gap in the DOS and a singularity at the upper edge. On the other hand, for a gap with the d-wave symmetry there are still allowed states at any energy around ε_F. The electronic DOS decreases continuously to zero when approaching ε_F. There is thus no gap in the strict sense for the DOS and the singularity at $2\Delta_{max}$ is damped [23]. It is important to notice that it is not only the presence of nodes in the gap function that determines the behaviour of phonon lines below T_c, but their localization in the Brillouin zone as well. As a consequence, for each symmetry of the gap the renormalization of phonons in the superconducting state will be different.

3.1. Analytical derivation

The total Hamiltonian of the system is given by

$$H = H_e + H_L + H_{eL} \quad . \tag{5}$$

The first two terms,

$$H_e + H_L = \sum_{\mathbf{k},\sigma} \varepsilon_{\mathbf{k}} c^{\dagger}_{\mathbf{k},\sigma} c_{\mathbf{k},\sigma} + \sum_{\nu,\mathbf{q}} \omega_{\nu\mathbf{q}} \left(b^{\dagger}_{\nu\mathbf{q}} b_{\nu\mathbf{q}} + \frac{1}{2} \right) \tag{6}$$

describe the zero-order Hamiltonian. H_e and H_L are the electronic and the lattice Hamiltonian, respectively. We consider here a single electronic band for simplicity, but the generalization is straightforward [18, 19]. The last part of the Hamiltonian is linear hole–lattice interaction

$$H_{eL} = \sum_{\mathbf{k}\sigma,\nu\mathbf{q}} g_{\nu}(\mathbf{k},\mathbf{q}) c^{\dagger}_{\mathbf{k},\sigma} c_{\mathbf{k}+\mathbf{q},\sigma} b^{\dagger}_{\nu\mathbf{q}} + h.c. \quad . \tag{7}$$

To calculate the superconductivity-induced renormalization of phonons one has to modify the Hamiltonian so as to include in the zeroth order the appearance of the gap. To this aim one adds to and subtracts from (5) the following terms [18]:

$$H_\Delta = \sum_{\mathbf{k}} \Delta_{\mathbf{k}} c^\dagger_{\mathbf{k}\uparrow} c^\dagger_{-\mathbf{k}\downarrow} + h.c. \quad , \tag{8}$$

$$H_\chi = \sum_{\mathbf{k},\sigma} \chi_{\mathbf{k}} c^\dagger_{\mathbf{k},\sigma} c_{\mathbf{k}\sigma} \quad , \tag{9}$$

$$\delta H_L = \sum_{\mathbf{q},\nu} \delta\omega_{\nu\mathbf{q}} b^\dagger_{\nu\mathbf{q}} b_{\nu\mathbf{q}} \quad , \tag{10}$$

$$\delta H_{eL} = \sum_{\mathbf{k},\sigma} \sum_{\nu\mathbf{q}} \delta g_\nu(\mathbf{k},\mathbf{q}) c^\dagger_{\mathbf{k},\sigma} c_{\mathbf{k}+\mathbf{q},\sigma} b^\dagger_{\nu\mathbf{q}} + h.c. \quad . \tag{11}$$

The first two terms describe the superconducting (gap) and Hartree–Fock mean-fields. The two next terms describe the renormalization of the phonon energy and of electron–phonon interaction. These are assumed to be second-order effects and can be considered as small. The new zero-order Hamiltonian can now be defined as

$$H_0 = H_{SC} + \bar{H}_L \quad , \tag{12}$$

where

$$\begin{aligned} H_{SC} &= H_e + H_\Delta + H_\chi - \mu N = \\ &= \sum_{\mathbf{k}} E_{\mathbf{k}} \left(a^\dagger_{1\mathbf{k}} a_{1\mathbf{k}} + a^\dagger_{2\mathbf{k}} a_{2\mathbf{k}} \right) \end{aligned} \tag{13}$$

and $\bar{H}_L = H_L + \delta H_L$ is the renormalized phonon Hamiltonian. The electronic part H_{SC} is written in its diagonal form by using the Bogolyubov operators a_1, a_2. The total Hamiltonian takes the form

$$H = H_0 + H', \tag{14}$$

$$H' = \bar{H}_{eL} - H_\Delta - H_\chi - \delta H_L + \delta H_{eL} \quad , \tag{15}$$

where $\bar{H}_{eL} = H_{eL} + \delta H_{eL}$. The unknowns $\Delta_{\mathbf{k}}$, $\chi_{\mathbf{k}}$, $\delta\omega_{\nu\mathbf{q}}$, and $\delta g_\nu(\mathbf{k},\mathbf{q})$ have to be determined in a self-consistent way [4, 18]. The zero-order Hamiltonian is chosen in such a way that it describes the superconducting state. Thus, first of all one has to eliminate the linear electron–lattice coupling. This is done with two unitary transformations. The first one is a polaron-type and the second one, a Fröhlich-type transformation. By applying them to (14) consecutively one obtains after some calculations two coupled equations for $\Delta_{\mathbf{k}}$, $\chi_{\mathbf{k}}$ (the BCS gap equation is a special case of them), an equation for $\delta g_\nu(\mathbf{k},\mathbf{q})$, and an expression for $\delta\omega_{\nu\mathbf{q}}$. This last function is obtained for any wavevector $\mathbf{q}$ of the phonon [18]. Here we

give its form only for $\mathbf{q} = 0$ which is the quantity measured in Raman experiments:

$$\delta\omega_{\nu 0} = -4 \sum_{\mathbf{k}} |\bar{g}_\nu(\mathbf{k}, 0)|^2 \frac{\Delta_{\mathbf{k}}^2 (1 - 2\bar{f}_{\mathbf{k}})}{E_{\mathbf{k}} \left[(2E_{\mathbf{k}})^2 - (\omega_{\nu 0})^2 \right]}. \tag{16}$$

This expression takes into account the anisotropy of the gap as well as the $\mathbf{k}$ dependence of the electron–lattice coupling. We are now able to study the influence of the symmetry of the superconducting gap on the renormalization of the phonon energy.

3.2. Numerical calculation

For the numerical study of renormalization we assume that the electron–lattice coupling is diagonal so that $\bar{g}_\nu(\mathbf{k}, \mathbf{q}) \equiv \bar{g}_\nu(\mathbf{q})$. Furthermore, we replace the sum in (16) by an integral and $\omega_{\nu 0}$, by a complex continuous variable $\omega + i\eta$. The resulting phonon renormalization will be complex: $\delta\omega_{\nu 0} = \Delta\omega_{\nu 0} + i\Delta\gamma_{\nu 0}$. The shift $\Delta\omega_{\nu 0}$ and the change of the linewidth $\Delta\gamma_{\nu 0}$ of a specific phonon is obtained for $\omega = \omega_{\nu 0}$. To calculate the gap function we choose for $V_{\mathbf{k}\mathbf{k}'}$ the pairing function which results from short-range distortive interaction (3) with $V_2 = 0$ and to which we add a constant term V_0. Within this model gaps with both d- and s-wave symmetries can be obtained as stable solutions depending on the value of the chemical potential $\mu = t\mu'$. Note that the main results presented below are independent of the special features of the model as shown in [18]. The structure of the pairing potential implies that the solutions of gap equation (1) have the form $\Delta_{\mathbf{k}} = \Delta_0 + \Delta_x \cos(k_x) + \Delta_y \cos(k_y)$. The terminology used for the symmetry of the gap is as follows: s-wave isotropic for $\Delta_0 \neq 0$, $\Delta_x = \Delta_y = 0$, s-wave anisotropic for $\Delta_x = \Delta_y \neq 0$, d-wave for $\Delta_0 = 0$, $\Delta_x = -\Delta_y \neq 0$, and mixed for $\Delta_0 \neq 0 \neq \Delta_x \neq \Delta_y$. The numerical calculations are carried out at $T = 0$ and the parameters V_0 and V_1 are always chosen so that $T_c = 90$ K. The results for the same two values of the chemical potential as for the calculation of the gap are discussed here. The choice $\mu' = -1.35$ is made to reproduce the Fermi surface of $YBa_2Cu_3O_7$. $\mu' = -2.22$ is then selected because T_c is 90 K for the same values of V_0 and V_1 as for $\mu' = -1.35$. In the former case the gap has a d-wave symmetry and in the latter one it has s-wave character.

Let us first look at the shift of the phonon lines in Fig. 5. The solid line is obtained for an isotropic pairing potential $V_{\mathbf{k}\mathbf{k}'} = V_0$. In contrast to the BCS model it has no energy cutoff. The form is nevertheless very similar to the BCS result which can be calculated analytically [24]. The only difference is that the singularity is now damped due to lifetime effects. The long dashed curve is obtained for an s-wave anisotropic gap and the last one (short dashed curve) results from the calculation with a d-wave anisotropic

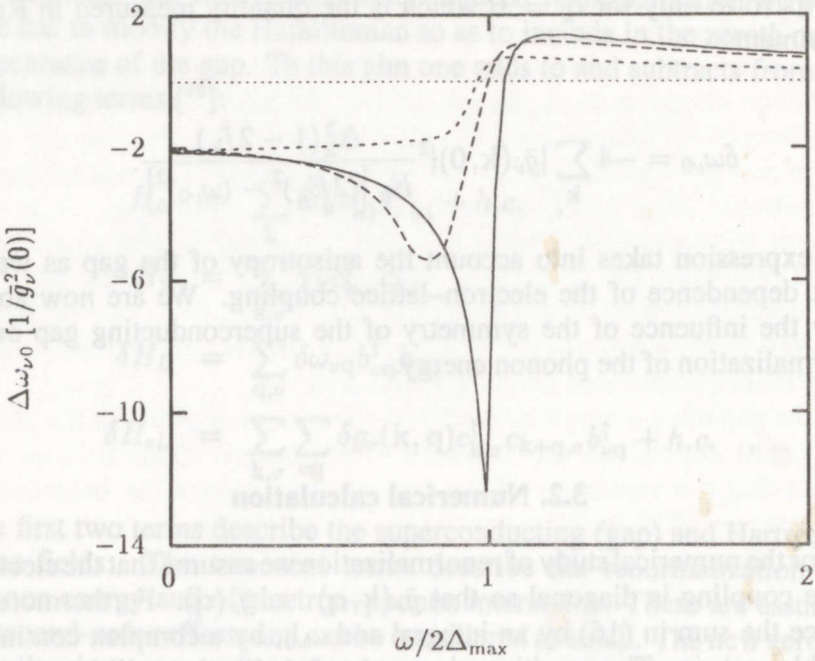

Fig. 5. Real part of $\delta\omega_{\nu 0}$ at $T = 0$ for an isotropic s-wave (solid line), an anisotropic s-wave (dashed line), and the anisotropic d-wave (short-dashed line) case. The respective parameters are (a) $V_0 = -0.248$, $V_1 = 0$, (b) $V_0 = V_1 = -0.15$ with $\mu' \simeq -2.22$, and (c) $V_0 = 0$, $V_1 = -0.299$ with $\mu' = -1.35$. $\Delta_{\max} = 17.6$ meV in each case.

gap function. The only feature common to all three curves is that phonons with the energy below $2\Delta_{\max}$ ($\approx$ 35 meV) are softened and those with a higher energy experience a hardening. Otherwise the curves are rather different. It has already been shown in [24] that the BCS model (and its extension – solid line) cannot reproduce Raman experiments. The maximal softening near $2\Delta_{\max}$ is much too large. In the d-wave case (short-dashed curve), on the contrary, *all* phonons below $2\Delta_{\max}$ show the same small softening. The anisotropy of the gap completely washes out the singularity. Finally, the phonon shifts obtained for an anisotropic s-wave gap is an intermediate situation between the two first ones. From the experimental point of view among the five Raman active modes observed in $YBa_2Cu_3O_7$ (at 115, 150, 340, 435, and 500 cm^{-1}) the two lowest in energy show no measurable renormalization, the 340 cm^{-1} mode is strongly softened and the two highest phonons harden below T_c. As a consequence, the gap cannot have a d-wave symmetry because the predicted softening is too small and all phonons below the 435 cm^{-1} mode should have the same softening. The result obtained with an s-wave anisotropy instead gives the right order of magnitude for the softenings.

The changes of linewidths below T_c corresponding to the three situations studied above are depicted in Fig. 6. Again one feature is common to all cases. The q = 0 phonon lines broaden and never narrow below T_c. There is one main difference between the s-wave- and the d-

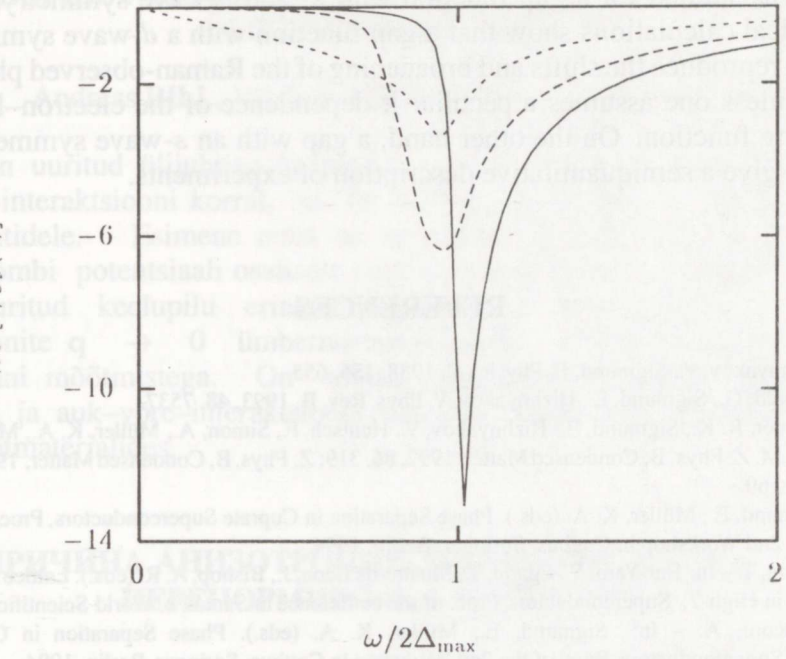

Fig. 6. The imaginary part of $\delta\omega_{\nu 0}$ at $T = 0$ corresponding to the three situations of Fig. 5.

wave-induced broadening. In the former case there is always an energy threshold below which the phonon line does not change. In the second case the broadening is finite already for low energy phonons. A comparison with experiments shows that a gap with a d-wave symmetry cannot reproduce the results since there is a clear threshold for the existence of a broadening of phonon lines. In fact there is even a small narrowing for the two lowest phonons that has to be attributed to the change of lattice properties upon lowering the temperature.

4. CONCLUSIONS

Based on the observation of lattice and electronic local inhomogeneities in cuprate superconductors, we have shown that there are two typical contributions to the electron–lattice interaction that distinguish these systems from conventional superconductors. One part is the distortive coupling inducing static distortions of the near surrounding of doped holes (short-range) and the other one is the nontotally screened long-range interaction. The structure of the gap function was calculated in the framework of the BCS theory for the two parts separately. The gap resulting from the long-range interaction for $\mu' = -1.35$ fits well the experimental determination of anisotropy. This k dependence can be seen to be a consequence of the structure of the electronic density of states. In a second step the renormalization of the phonon energy due to the superconducting

state was studied for a gap function with s- and d-wave symmetry. The numerical calculations show that a gap function with a d-wave symmetry cannot reproduce the shifts and broadening of the Raman-observed phonon lines unless one assumes a peculiar k dependence of the electron–lattice coupling function. On the other hand, a gap with an s-wave symmetry is able to give a semiquantitative description of experiments.

REFERENCES

1. Hizhnyakov, V., Sigmund, E. Physica C, 1988, **156**, 655.
2. Seibold, G., Sigmund, E., Hizhnyakov, V. Phys. Rev. B, 1993, **48**, 7537.
3. Kremer, R. K., Sigmund, E., Hizhnyakov, V., Hentsch, F., Simon, A., Müller, K. A., Mehring, M. Z. Phys. B, Condensed Matter, 1992, **86**, 319; Z. Phys. B, Condensed Matter, 1993, **91**, 169.
4. Sigmund, E., Müller, K. A. (eds.). Phase Separation in Cuprate Superconductors, Proc. of the 2nd Workshop in Cottbus. Springer, Berlin, 1994.
5. Egami, T. – In: Bar-Yam, Y., Egami, T., Mustre-de Leon, J., Bishop, A. R. (eds.). Lattice Effects in High-T_c Superconductors, Proc. of the conference in Santa Fe. World Scientific, 1992.
6. Bianconi, A. – In: Sigmund, E., Müller, K. A. (eds.). Phase Separation in Cuprate Superconductors, Proc. of the 2nd Workshop in Cottbus. Springer, Berlin, 1994.
7. Hammel, P. C. – In: Müller, K. A., Benedek, G. (eds.). Phase Separation in Cuprate Superconductors, Proc. of the 1st Workshop in Erice. World Scientific, Singapore, 1993; Sigmund, E., Müller, K. A. (eds.). Phase Separation in Cuprate Superconductors, Proc. of the 2nd Workshop in Cottbus. Springer, Berlin, 1994.
8. Hizhnyakov, V., Sigmund, E., Seibold, G. – In: Müller, K. A., Benedek, G. (eds.). Phase Separation in Cuprate Superconductors, Proc. of the 1st Workshop in Erice. World Scientific, Singapore, 1993; Sigmund, E., Müller, K. A. (eds.). Phase Separation in Cuprate Superconductors, Proc. of the 2nd Workshop in Cottbus. Springer, Berlin, 1994.
9. Müller, K. A., Benedek, G. (eds.). Phase Separation in Cuprate Superconductors, Proc. of the 1st Workshop in Erice. World Scientific, Singapore, 1993.
10. Jorgensen, J. D. – In: Bar-Yam, Y., Egami, T., Mustre-de Leon, J., Bishop, A. R. (eds.). Lattice Effects in High-T_c Superconductors, Proc. of the conference in Santa Fe. World Scientific, 1992.
11. Goodenough, J. B., Zhou, J.-S. – In: Mihailovic, D., Müller, K. A. (eds.). Anharmonic Properties of High-T_c Cuprates. World Scientific, 1995.
12. Shen, Z.-X., Dessau, D. S., Wells, B. O., King, D. M., Spicer, W. E., Arko, A. J., Marshall, D., Lombardo, L. W., Kapitulnik, A., Dickinson, P., Doniach, S., DiCarlo, J., Loeser, A. G., Park, C. H. Phys. Rev. Lett., 1993, **70**, 1553.
13. Deutscher, G. – In: Sigmund, E., Müller, K. A. (eds.). Phase Separation in Cuprate Superconductors, Proc. of the 2nd Workshop in Cottbus. Springer, Berlin, 1994.
14. Campuzano, J. C., Jennings, G., Faiz, M., Beaulaigue, L., Veal, B. W., Liu, J. Z., Paulikas, A. P., Vandervoot, K., Claus, H. Phys. Rev. Lett., 1990, **64**, 2308.
15. Chakravarty, S., Sudbo, A., Anderson, P. W., Strong, S. Science, 1993, **261**, 337.
16. Schneider, T., Soerensen, S. Z. Phys. B, 1990, **81**, 3.
17. Eremin, V. H., private communication.
18. Bill, A., Hizhnyakov, V., Sigmund, E. Physica C, Dec. 1994; Bill, A., Hizhnyakov, V., Sigmund, E., submitted to Phys. Rev. B; Bill, A. PhD Thesis, Stuttgart, 1994 (unpublished).
19. Hizhnyakov, V., Sigmund, E. Phys. Rev. B. (to be published).
20. Monthoux, P., Balatsky, A. V., Pines, D. Phys. Rev. Lett., 1991, **67**, 3448.
21. Li, Q. P., Joynt, R. Phys. Rev. B, 1993, **47**, 530.
22. Friedl, B., Thomsen, C., Cardona, M. Phys. Rev. Lett., 1990, **65**, 915.
23. Spathis, P. N., Soerensen, M. P., Lazarides, N. Phys. Rev. B, 1992, **45**, 7360.
24. Zeyher, R., Zwicknagel, G. Z. Phys. B, Condensed Matter, 1990, **78**, 175.

KEELUPILU ANISOTROOPIA TEKKEPÕHJUS JA FOONONITE ÜMBERNORMEERUMINE

Andreas BILL, Vladimir HIŽNJAKOV, Ernst SIGMUND

On uuritud ülijuhtiva keelupilu anisotroopiat kahe erisuguse auk–võre–interaktsiooni korral, mis on iseloomulikud kõrgtemperatuursetele ülijuhtidele. Esimene neist on moonutav lähimõju seos ja teine on Coulombi potentsiaali osalisest varjestamisest tingitud kaugmõju. Edasi on uuritud keelupilu erineva sümmeetria (s-laine, d-laine ...) mõju foononite $\mathbf{q} \rightarrow 0$ ümbernormeerumisele. Tulemusi on võrreldud Ramani mõõtmistega. On tehtud järeldused keelupilu sümmeetria kohta ja auk–võre–interaktsiooni tugevuse kohta kõrgtemperatuursetes ülijuhtmaterjalides.

ПРИЧИНА АНИЗОТРОПИИ ЗАПРЕТНОЙ ЗОНЫ И ПЕРЕНОРМИРОВКА ФОНОНОВ

Андреас БИЛЛ, Владимир ХИЖНЯКОВ, Эрнст ЗИГМУНД

Изучена анизотропия сверхпроводящей щели для двух видов элекрон-фононного взаимодействия, существенных для высокотемпературных сверхпроводников. Первое учитывает близкодействующее деформационное влияние, второе – дальнодействующее влияние, обусловленное неполным экранированием кулоновского потенциала. Исследовано влияние симметрии щели (s-волновой, d-волновой...) на перенормировку $\mathbf{q} \rightarrow 0$ фононов. Результаты сравниваются с экспериментальными данными по комбинационному рассеянию. Приведены выводы, касающиеся симметрии щели и силы электрон-фононного взаимодействия в высокотемпературных сверхпроводниках.